Counting statistics in nanoscale junctions

Yu-Shen Liu and Yu-Chang Chen*

Department of Electrophysics, National Chiao Tung University, 1001 Ta Hush Road, Hsinchu 30010, Taiwan

(Received 22 September 2010; revised manuscript received 16 November 2010; published 3 January 2011)

We present first-principles calculations for moments of the current up to the third order in atomic-scale junctions. The quantum correlations of the current are calculated using the current operator in terms of the wave functions obtained self-consistently within the static density-functional theory. We investigate the relationships of the conductance, the second, and the third moment of the current for carbon atom chains of various lengths bridging two metal electrodes in the linear and nonlinear regimes. The conductance, the second-, and the third-order Fano factors exhibit odd-even oscillation with the number of carbon atoms due to the full and half filled π^* orbital near the Fermi levels. The third-order Fano factor and the conductance are positively correlated.

DOI: 10.1103/PhysRevB.83.035401 PACS number(s): 73.63.Rt, 72.10.Bg, 73.21.Hb, 74.40.De

I. INTRODUCTION

The field of nanoscale electronics has generated a tremendous wave of scientific interest in the past decade due to prospects of device-size reduction offered by atomic-level control of certain physical properties.[1] The field has also spurred great interest in the fundamental understanding of quantum transport.[2] One of the fundamental questions in quantum transport relates to moments of the current. For instance, the second moment—shot noise—defines the quantum fluctuations of the current at zero temperature due to the quantization of charge. Shot noise can be expressed as $S_2 \propto \sum_n T_n (1 - T_n)$ in terms of the transmission probabilities of each eigenchannel T_n.[3] Shot noise reaches the classical limit $2eI$, where e is the electron charge and I is the average current, when electrons in a conductor drift in a completely uncorrelated way, as described by a Poissonian distribution of current events.[4]

Studying steady-state current fluctuations can provide fundamental insight into the nature of electron transport, including the role of the Pauli exclusion principle and the statistics of quantized charge. Unlike the temperature-dependent thermal noise (Johnson-Nyquist noise), shot noise depends on properties of the underlying transport process. In a mesoscopic system, the size of the junction is larger than the dephasing length, thus electrons relevant in transport can lose coherence in phase via multiple scattering. In this case, the current operator is typically expressed in terms of the scattering matrix, where the transverse quantum channels are restored via adiabatic constriction.[3] Interference effects between channels are typically small and negligible.[5] However, the transport mechanism in atomic-scale junctions is different from that in a mesoscopic system. The atomic junctions are small, such that electron tunneling in the junction is coherent. Consequently, the current operator of atomic junctions can be expressed in terms of wave functions. The wave nature of the current operator in terms of wave functions may lead to interference in the quantum correlation of currents. This motivates exploration of the quantum interference effects on moments of the current due to the wave nature of the current operator in atomic junctions. This paper shows that wave functions with different **K** channels are correlated with one another in the calculations of shot noise and the third moment of the current.

Shot noise in atomic and molecular junctions has been addressed via experiments,[6–9] model calculations,[10–12] and first-principles calculations.[13–16] Shot noise depends on detailed electronic distributions, thus it provides a sensitive tool for probing nanojunctions, where detailed electronic structures can be affected by the exact arrangement of individual atoms.[14] Shot noise may provide a nondestructive way to explore the local temperatures of nanostructures caused by the coupling of propagating electrons and ionic vibrations.[15] In fact, it has been employed in recent experiments to characterize the signature of molecular or atomic junctions.[6,7,17,18]

No studies are known to have considered higher moments of the current in atomic-scale systems while accounting for the effect of detailed electronic structures from first principles. To address this issue, we develop a theoretical approach starting from the current operator in terms of wave functions calculated self-consistently in the framework of static density-functional theory (DFT). It allows us to compute quantum correlations of the steady-state current relevant to the interference of the current operator in terms of wave functions up to the third moment. The higher moments of the current, although more difficult to measure and calculate, provide deeper insight into the interference effect due to the wave nature of the current operator in atomic-scale junctions. These are more elaborate tools for exploring higher-order quantum correlations of quantized electrons. The third moment of the current describes the correlation of third-order current fluctuations in the time domain. Due to the complex mixing of the product of wave functions with different transverse momenta **K** channels, the third moment of the current may render additional information on the quantum interference effects. Measurement of the third-order current correlators requires three detectors to distinguish the signal locally and avoid the back action of nanojunctions.

In atomic and molecular junctions, moments of the current are closely related to the detailed electronic structures. First-principles calculations provide information regarding the connection between the detailed electronic structures and moments of the current with no adjustable parameters that go beyond what the model calculations can provide. This point is demonstrated through a prototypical nanojunction consisting of an atomic chain with different numbers of carbon atoms connecting two metal electrodes [Fig. 1(a)]. The first (current), the second (shot noise, S_2), and the third

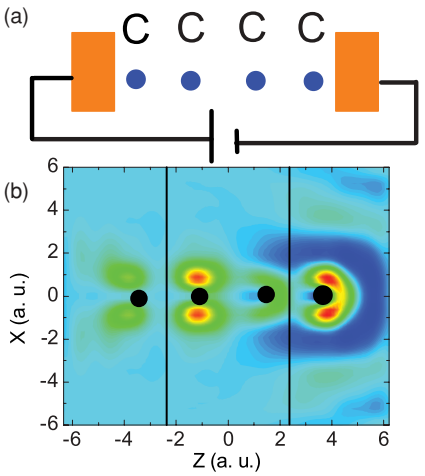

FIG. 1. (Color online) (a) Schematic of the four-carbon atomic junction. (b) The spacial distribution of partial charge density for electrons with energies near the Fermi levels shows π^*-orbital characters at $V_B = 0.01$ V. Vertical black lines correspond to the edges of the jellium model and circles correspond to atomic position.

moment (S_3) of the current are investigated. The carbon atom chain is not merely an academic example because carbon is a versatile element capable of forming diverse structures, including diamond, graphite, fullerenes, nanotubes, and graphene. Recently, experiments have demonstrated the possibility of forming carbon atomic chains from graphite using transmission electron microscopy.[19] In this regard, they are among the few model systems in which theory and experiments can be reasonably compared. Carbon atom chains have regularly patterned electronic structures as a function of the number of carbon atoms.[20] Patterned electronic structures serve as ideal test beds for studying relationships among moments of the current, which are sensitively related to the detailed electronic structures of nanojunctions.

II. THEORETICAL METHODS

First-principles calculations are performed for the atomic chains with different numbers of carbon atoms connecting to two semi-infinite metal electrodes in the framework of density-functional theory. The full Hamiltonian of the system is $H = H_0 + V$, where H_0 is the Hamiltonian due to the bare electrodes modeled as electron jellium separated by a distance and V is the scattering potential of the nanostructured object bridging the semi-infinite electrodes with a planar surface.

Wave functions of the unperturbed Hamiltonian due to the bimetallic junction with an applied bias [$V_B = (\mu_R - \mu_L)/e$, where $\mu_{L(R)}$ is the chemical potential deep in the left (right) electrode] are computed. The unperturbed wave functions have the form $\Psi_{E\mathbf{K}}^{0,L(R)}(\mathbf{r}) = (2\pi)^{-1} e^{i\mathbf{K}\cdot\mathbf{R}} \cdot u_{E\mathbf{K}}^{L(R)}(z)$, where $u_{E\mathbf{K}}^{L(R)}(z)$ is the wave function of the bare electrodes along the z direction before inclusion of the nanostructured object. The equation $u_{E\mathbf{K}}^{L(R)}(z)$ is calculated by solving the coupled Shrödinger and Poisson equations iteratively until self-consistency is reached. Deep inside the electrodes ($z \to \pm\infty$), the right- and left-moving waves satisfy the scattering boundary conditions,

$$u_{E\mathbf{K}}^{L}(z) = \sqrt{\frac{m}{2\pi\hbar^2 k_L}} \times \begin{cases} e^{ik_L z} + R_L e^{-ik_L z}, & z < -\infty \\ T_L e^{ik_R z}, & z > \infty \end{cases} \quad (1)$$

and

$$u_{E\mathbf{K}}^{R}(z) = \sqrt{\frac{m}{2\pi\hbar^2 k_R}} \times \begin{cases} T_R e^{-ik_L z}, & z < -\infty \\ e^{-ik_R z} + R_R e^{ik_R z}, & z > \infty, \end{cases} \quad (2)$$

where $\mathbf{K}$ is the electron momentum in the plane parallel to the electrode surfaces, and z is the coordinate parallel to the direction of the current. The condition of energy conservation gives $\frac{\hbar^2 k_R^2}{2m} = E - \frac{\hbar^2 \mathbf{K}^2}{2m} - v_{\text{eff}}(\infty)$ and $\frac{\hbar^2 k_L^2}{2m} = E - \frac{\hbar^2 \mathbf{K}^2}{2m} - v_{\text{eff}}(-\infty)$, where $v_{\text{eff}}(z)$ is the effective potential comprising the electrostatic potential and exchange correlation energy. Note that $v_{\text{eff}}(\pm\infty)$ are the bottom of the conduction band deep inside the right and left electrodes.

Inclusion of the nanostructured object is considered in the scattering approach. The wave functions of the total system (bimetallic junction + atom or molecule) are calculated by solving the Lippmann-Schwinger equation iteratively until self-consistency is reached,

$$\Psi_{E\mathbf{K}}^{L(R)}(\mathbf{r}) = \Psi_{E\mathbf{K}}^{0,L(R)}(\mathbf{r}) + \int d^3\mathbf{r}_1 \int d^3\mathbf{r}_2 G_E^0(\mathbf{r},\mathbf{r}_1) V(\mathbf{r}_1,\mathbf{r}_2) \Psi_{E\mathbf{K}}^{L(R)}(\mathbf{r}_2), \quad (3)$$

where $\Psi_{E\mathbf{K}}^{L(R)}(\mathbf{r})$ stands for the effective single-particle wave functions of the entire system, corresponding to propagating electrons incident from the left (right) electrode. The quantity G_E^0 is the Green's function for the bimetallic junction. The potential $V(\mathbf{r}_1,\mathbf{r}_2)$ that electrons experience when they scatter through the nanojunction is

$$V(\mathbf{r}_1,\mathbf{r}_2) = V_{ps}(\mathbf{r}_1,\mathbf{r}_2) + \left\{ \left(V_{xc}\left[n\left(\mathbf{r}_1\right)\right] - V_{xc}\left[n_0\left(\mathbf{r}_1\right)\right] \right) + \int d\mathbf{r}_3 \frac{\delta n\left(\mathbf{r}_3\right)}{|\mathbf{r}_1 - \mathbf{r}_3|} \right\} \delta(\mathbf{r}_1 - \mathbf{r}_2), \quad (4)$$

where $V_{ps}(\mathbf{r}_1,\mathbf{r}_2)$ is the electron-ion interaction potential,[21] $n_0(\mathbf{r})$ is the electron density for the pair of biased bare electrodes, $n(\mathbf{r})$ is the electron density for the total system, and $\delta n(\mathbf{r})$ is their difference. The quantity G_E^0 is the Green's function for the bimetallic junction, $V_{xc}[n(\mathbf{r})]$ is the exchange-correlation potential calculated at the level of local-density approximation. We note that the external bias [$V_B = (\mu_R - \mu_L)/e$] is considered in the bimetallic junction with different chemical potential deep in the electrodes. When a molecule is included in the junction, the Lippmann-Schwinger equation is applied to calculate wave functions of the entire system (electrodes + molecule) until self-consistency is achieved. Thus the high-bias case is considered and calculated on the same footing as the zero-bias case using the Lippmann-Schwinger equation.

Chemical potentials deep in the electrodes are maintained by the external bias. The electrode-molecule-electrode system is considered as a unified coherent quantum system. The group of atoms introduced between the electrodes are enclosed in

a box that includes part of the electrodes. The simulation box is sufficiently large that the charge density outside the box is unperturbed by the introduction of a group of atoms. Bases of 2300–3500 plane waves have been chosen for different lengths of carbon atom chains in this study. Localized states are solved by directly diagonalizing the Hamiltonian. More detailed descriptions of the theory can be found in Refs. 22 and 23.

The quantum transport theory based on the combination of DFT and the Lippmann-Schwinger equation in the scattering approach is equivalent to the theory based on a combination of DFT and the nonequilibrium Green's function.[24] For weakly coupled systems such as a molecule weakly adsorbed to electrodes, self-interaction errors may be significant. More elaborate consideration of exchange-correlation energy is an important ingredient in providing accurate quantitative descriptions in molecular transport calculations.[25] The correction to the exchange-correlation kernel due to the Vignale-Kohn approximation in time-dependent current-density-functional theory (TDCDET) is also important in the weakly adsorbed case.[26] The viscous nature of the electron liquid is more important for the molecular junction than for the quantum point contacts.[27] The reason for this is that the correction due to the dynamical corrections depends nonlinearly on the gradient of the electron density. For strongly coupled systems, such as monatomic chains described in this study, the exchange correlation in local-density approximation, which neglects the dynamical corrections, is remarkably successful when compared to the experiments.

A. Second moment of the current shot noise

We define a field operator describing propagating electrons incident from the left and right electrodes in terms of $\Psi^{L(R)}_{E\mathbf{K}}(\mathbf{r})$ with energy E and $\mathbf{K}$ as the eigenstate. The component of momenta $\mathbf{K}$ parallel to the electrode surface serves as the quantum channels. The field operator is

$$\hat{\Psi} = \sum_{\alpha,E,\mathbf{K}} a^{\alpha}_{E\mathbf{K}}(t)\,\Psi^{\alpha}_{E\mathbf{K}}(\mathbf{r}), \tag{5}$$

where $\alpha = L$ or R, $a^{L(R)}_{E\mathbf{K}}(t) = \exp(-i\omega t)a^{L(R)}_{E\mathbf{K}}$, and $a^{L(R)}_{E\mathbf{K}}$ is the annihilation operators of electrons incident from the left (right) reservoir, satisfying the anticommutation relations,

$$\left\{a^{\alpha}_{E_1\mathbf{K}_1}, a^{\beta\dagger}_{E_2\mathbf{K}_2}\right\} = \delta_{\alpha\beta}\delta(E_1 - E_2)\,\delta(\mathbf{K}_1 - \mathbf{K}_2), \tag{6}$$

where $\beta = L$ or R.

The expectation value of the product of electron creation and annihilation operator at thermal equilibrium is given by

$$\left\langle a^{\alpha\dagger}_{E_1\mathbf{K}_1} a_{E_2\mathbf{K}_2}\right\rangle^{\beta} = \delta_{\alpha\beta}\delta(E_1 - E_2)\,\delta(\mathbf{K}_1 - \mathbf{K}_2) f^{\alpha}_{E}, \tag{7}$$

where the statistics of electrons coming from the left (right) electrodes are determined by the equilibrium Fermi-Dirac distribution function $f^{L(R)}_{E} = 1/\{1 + \exp[(E - \mu_{L(R)})/(k_B T)]\}$ in the left (right) reservoir.

We introduce the current operator with the field operator in terms of wave functions,

$$\hat{I}(z,t) = \frac{e\hbar}{mi}\int d\mathbf{r}_{\perp}\int \mathbf{dK_1}\int \mathbf{dK_2}[\hat{\Psi}^{\dagger}\nabla\hat{\Psi} - \nabla\hat{\Psi}^{\dagger}\hat{\Psi}], \tag{8}$$

where $\hat{\Psi}$ is the field operator described in Eq. (5). Equation (8) can be expressed alternatively as

$$\hat{I}(z,t) = \frac{e\hbar}{mi}\sum_{E_1E_2}\sum_{\alpha\beta}\int d\mathbf{r}_{\perp}\int d\mathbf{K}_1\int d\mathbf{K}_2 \times e^{i(E_1-E_2)t/\hbar}a^{\alpha\dagger}_{E_1\mathbf{K}_1}a^{\beta}_{E_2\mathbf{K}_2}\tilde{I}^{\alpha\beta}_{E_1\mathbf{K}_1,E_2\mathbf{K}_2}(\mathbf{r}), \tag{9}$$

where $\tilde{I}^{\alpha\beta}_{E_1\mathbf{K}_1,E_2\mathbf{K}_2}(\mathbf{r}) = (\Psi^{\alpha}_{E_1\mathbf{K}_1})^{*}\nabla\Psi^{\beta}_{E_2\mathbf{K}_2} - \nabla(\Psi^{\alpha}_{E_1\mathbf{K}_1})^{*}\Psi^{\beta}_{E_2\mathbf{K}_2}$.

The average of the current at zero temperature is given by

$$\langle\hat{I}(z)\rangle = \frac{e\hbar}{mi}\int_{E_{FL}}^{E_{FR}} dE\int d\mathbf{r}_{\perp}\int d\mathbf{K}\tilde{I}^{R,R}_{E\mathbf{K},E\mathbf{K}}(\mathbf{r}), \tag{10}$$

where Eq. (7) is applied to calculate the expectation of Eq. (9). Equation (10) is exactly the same as the current described by the first quantization. Note that $\langle\hat{I}(z)\rangle$ is independent of z for a steady-state current. The averaged current also lacks the overlap integral of wave functions with different transverse momenta $\mathbf{K}$.

The shot-noise spectral function is defined as

$$S_2(\omega,T;\,z_1,z_2) = 2\pi\hbar\int d(t_1 - t_2)\,e^{i\omega(t_1-t_2)}\langle\Delta\hat{I}(z_1,t_1)\Delta\hat{I}(z_2,t_2)\rangle, \tag{11}$$

where $\Delta\hat{I}(t) = \hat{I}(t) - \langle\hat{I}\rangle$. Carrying out the average of autocorrelation of the current operators requires the quantum statistical expectation value of the products of $a^{i\dagger}_{E_1}a^{j}_{E_2}a^{k\dagger}_{E_3}a^{l}_{E_4}$. For a Fermi electron gas at equilibrium, the quantum statistical expectation values of products of four operators are given by

$$\left\langle a^{i\dagger}_{E_1\mathbf{K}_1}a^{j}_{E_2\mathbf{K}_2}a^{k\dagger}_{E_3\mathbf{K}_3}a^{l}_{E_4\mathbf{K}_4}\right\rangle = \left\langle a^{i\dagger}_{E_1\mathbf{K}_1}a^{j}_{E_2\mathbf{K}_2}\right\rangle\left\langle a^{k\dagger}_{E_3\mathbf{K}_3}a^{l}_{E_4\mathbf{K}_4}\right\rangle - \left\langle a^{i\dagger}_{E_1\mathbf{K}_1}a^{l}_{E_4\mathbf{K}_4}\right\rangle\left\langle a^{j}_{E_2\mathbf{K}_2}a^{k\dagger}_{E_3\mathbf{K}_3}\right\rangle. \tag{12}$$

Applying Eq. (12) to Eq. (11), the shot-noise spectral function is given by

$$S(\omega,T;z_1,z_2) = 2\pi\hbar\left(\frac{e\hbar}{mi}\right)^2\sum_{\alpha,\beta=L,R}\int dE f^{\alpha}_{E+\hbar\omega}\left(1 - f^{\beta}_{E}\right) \times\int d\mathbf{r}_{1\perp}\int d\mathbf{r}_{2\perp}\int d\mathbf{K}_1\int d\mathbf{K}_2\tilde{I}^{\alpha\beta}_{E+\hbar\omega\mathbf{K}_1,E\mathbf{K}_2}(\mathbf{r}_1) \times\tilde{I}^{\beta\alpha}_{E\mathbf{K}_1,E+\hbar\omega\mathbf{K}_2}(\mathbf{r}_2), \tag{13}$$

where $\tilde{I}^{\alpha\beta}_{E+\hbar\omega\mathbf{K}_1,E\mathbf{K}_2}(\mathbf{r}) = -[\tilde{I}^{\beta\alpha}_{E\mathbf{K}_1,E+\hbar\omega\mathbf{K}_2}(\mathbf{r})]^{*}$.

Shot noise is the quantum fluctuation of current autocorrelation at zero temperature due to the charge quantization. For a dc steady current, the shot noise is given by the noise spectral function at $\omega = 0$ and $T = 0$ K [i.e., $S_2 = S_2(\omega = 0, T = 0)$], which gives

$$S_2(z_1,z_2) = 2\pi\hbar\left(\frac{e\hbar}{mi}\right)^2\int_{E_{FL}}^{E_{FR}} dE\int d\mathbf{r}_{1\perp}\int d\mathbf{r}_{2\perp}\int d\mathbf{K}_1 \times\int d\mathbf{K}_2\tilde{I}^{RL}_{E\mathbf{K}_1,E\mathbf{K}_2}(\mathbf{r}_1)\tilde{I}^{LR}_{E\mathbf{K}_2,E\mathbf{K}_1}(\mathbf{r}_2). \tag{14}$$

Equation (14) leads to the relationship $S_2^{RR} = S_2^{LL} = -S_2^{LR} = -S_2^{RL}$, where $S_2^{RR} = S_2(z_1 \to \infty, z_2 \to \infty)$, $S_2^{LL} = S_2(z_1 \to -\infty, z_2 \to -\infty)$, $S_2^{LR} = S_2(z_1 \to -\infty, z_2 \to \infty)$, and $S_2^{RL} = S_2(z_1 \to \infty, z_2 \to -\infty)$, all of which are consequences of current conservation.

B. Third moment of the current

Unlike the formalism developed in Ref. 3, which has in-out ordering, the current operator defined in Eq. (5) describes a steady-state current in which time ordering is not involved. Therefore the third moment of the current is defined in the time-unordered way (this does not affect the second moment, however, it is important for the third and higher moments),

$$S_3(\omega,\omega';z_1,z_2,z_3) = \int d(t_1-t_3)\int d(t_2-t_3)e^{i\omega(t_1-t_3)}e^{i\omega'(t_2-t_3)} \times \langle \Delta\hat{I}(z_1,t_1)\Delta\hat{I}(z_2,t_2)\Delta\hat{I}(z_3,t_3)\rangle, \quad (15)$$

where $\Delta\hat{I}(t) = \hat{I}(t) - \langle\hat{I}\rangle$.

The spectral function of the third moment is given by

$$S_3(\omega,\omega';z_1,z_2,z_2) = (2\pi\hbar)^2\left(\frac{e\hbar}{mi}\right)^3\int_{E_{FL}}^{E_{FR}} dE\int d\mathbf{r}_{1\perp}\int d\mathbf{r}_{2\perp}\int d\mathbf{r}_{3\perp}\int d\mathbf{K}_1\int d\mathbf{K}_2\int d\mathbf{K}_3 \times \sum_{\alpha,\beta,\gamma=L,R}\Big[f_E^\alpha\big(1-f_{E+\hbar\omega}^\beta\big)\big(1-f_{E+\hbar\omega+\hbar\omega'}^\gamma\big)\cdot\tilde{I}^{\alpha\beta}_{E\mathbf{K}_1(E+\hbar\omega)\mathbf{K}_2}(\mathbf{r}_1)\tilde{I}^{\beta\gamma}_{(E+\hbar\omega)\mathbf{K}_2(E+\hbar\omega+\hbar\omega')\mathbf{K}_3}(\mathbf{r}_2)\tilde{I}^{\gamma\alpha}_{(E+\hbar\omega+\hbar\omega')\mathbf{K}_3E\mathbf{K}_1}(\mathbf{r}_3) - f_E^\alpha f_{E-\hbar\omega}^\beta\big(1-f_{E+\hbar\omega}^\gamma\big)\tilde{I}^{\alpha\gamma}_{E\mathbf{K}_1(E+\hbar\omega)\mathbf{K}_2}(\mathbf{r}_1)\tilde{I}^{\beta\alpha}_{(E-\hbar\omega')\mathbf{K}_2E\mathbf{K}_3}(\mathbf{r}_2)\tilde{I}^{\gamma\beta}_{(E+\hbar\omega)\mathbf{K}_3(E-\hbar\omega')\mathbf{K}_1}(\mathbf{r}_3)\Big], \quad (16)$$

where the quantum statistic expectation value of $\langle\Delta\hat{I}(z_1,t_1)\Delta\hat{I}(z_2,t_2)\Delta\hat{I}(z_3,t_3)\rangle$ is evaluated using the Wick–Bloch–De Dominicis theorem,[28]

$$\langle\hat{A}_n\hat{A}_{n-1}\cdots\hat{A}\rangle_1 = \begin{cases} 0, & \text{for } n = \text{odd}, \\ \sum_{m=1}^{n-1}\eta^{n-m-1}\langle\hat{A}_n\hat{A}\rangle_m\langle\hat{A}_{n-1}\cdots\hat{A}_{m+1}\hat{A}_{m-1}\cdots\hat{A}\rangle_1, & \text{for } n = \text{even}, \end{cases} \quad (17)$$

where $\hat{A}_i$ denotes either creation or annihilation operators and $\eta = -1(1)$ for fermions (bosons). Similarly, the third moment of the steady-state current at zero temperature and zero frequency [defined as $S_3 = S_3(\omega = 0,\omega' = 0,T = 0)$] is given by

$$S_3(z_1,z_2,z_2) = (2\pi\hbar)^2\left(\frac{e\hbar}{mi}\right)\int_{E_{FL}}^{E_{FR}} dE\int d\mathbf{r}_{1\perp}\int d\mathbf{r}_{2\perp}\int d\mathbf{r}_{3\perp}\int d\mathbf{K}_1\int d\mathbf{K}_2\int d\mathbf{K}_3 \Big[\tilde{I}^{RL}_{E\mathbf{K}_1E\mathbf{K}_2}(\mathbf{r}_1)\tilde{I}^{LL}_{E\mathbf{K}_2E\mathbf{K}_3}(\mathbf{r}_2)\tilde{I}^{LR}_{E\mathbf{K}_3E\mathbf{K}_1}(\mathbf{r}_3) - \tilde{I}^{RL}_{E\mathbf{K}_1E\mathbf{K}_3}(\mathbf{r}_1)\tilde{I}^{RR}_{E\mathbf{K}_2E\mathbf{K}_1}(\mathbf{r}_2)\tilde{I}^{LR}_{E\mathbf{K}_3E\mathbf{K}_2}(\mathbf{r}_3)\Big]. \quad (18)$$

We note that alternative definitions of the Fourier transform, e.g., the integrals with respect to $(t_1 - t_2)$ and $(t_2 - t_3)$ in Eq. (15), will lead to different parametrizations of frequencies ω and ω' in the spectral function [Eq. (16)]. However, for the steady-state current where $\omega = \omega' = 0$, the third moment at zero temperature and zero frequency is independent of the choices of the Fourier transform. Similar to the relationship $S_2^{RR} = S_2^{LL} = -S_2^{LR} = -S_2^{RL}$ for shot noise, the third moment of the current [Eq. (18)] leads to

$$S_3^{R(R,L)R} = S_3^{L(R,L)L} = -S_3^{L(R,L)R} = -S_3^{R(R,L)L}, \quad (19)$$

all of which are consequences of current conservation.

III. RESULTS AND DISCUSSION

Finding moments of the current requires the quantum statistical expectation values of the products of operators that create and annihilate electrons related to the statistics of quantized charge, as described in Eqs. (12) and (17). The spectral functions of moments of the current [Eqs. (13) and (16)] are simplified to Eqs. (14) and (18) in the limit of zero frequency and zero temperature due to the Pauli-exclusion principle, which is related to the factor $f_E^\alpha(1 - f_E^\beta)$.

As shown in Eq. (10), the expectation value of the current does not involve the spatial integral of the product of wave functions labeled with different transverse momenta $\mathbf{K}$. This is in contrast to shot noise [Eq. (14)] and the third moment of the current [Eq. (18)], in which the integrals over space mix up the products of wave functions labeled with different transverse momenta $\mathbf{K}$. Thus interference between wave functions with different momenta $\mathbf{K}$ is relevant in the second and third moments of the current.

To illustrate the role of interference effects among the transverse channels $\mathbf{K}$, we tentatively assume that the wave functions could be decomposed into the product of the transverse and longitudinal components, $\Psi^\alpha_{E,\mathbf{K}}(\mathbf{r}) = \chi_{\mathbf{K}}(\mathbf{r}_\perp)\,u^\alpha_{E\mathbf{K}}(z)$, where $\chi_{\mathbf{K}}(\mathbf{r}_\perp)$ is the transverse wave function satisfying the following orthonormal conditions:

$$\int d\mathbf{r}_\perp\chi^*_{\mathbf{K}_1}(\mathbf{r}_\perp)\,\chi_{\mathbf{K}_2}(\mathbf{r}_\perp) = \delta(\mathbf{K}_1 - \mathbf{K}_2), \quad (20)$$

and $u^\alpha_{E\mathbf{K}}(z)$ presents the wave function along the z direction satisfying the boundary conditions given by Eqs. (1) and (2). If the wave functions are plugged into Eqs. (10) and (14), the

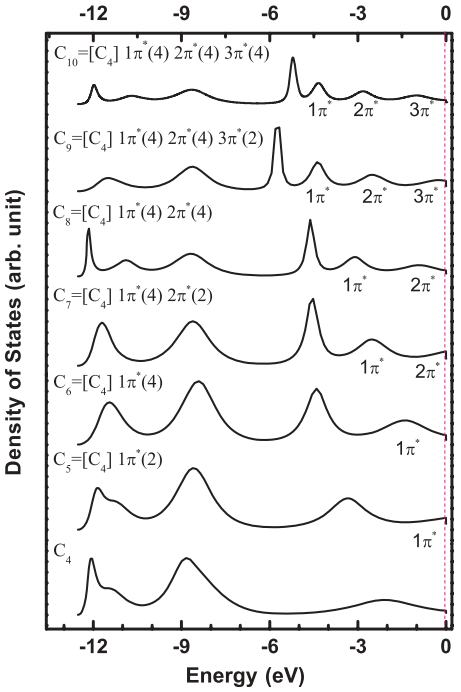

FIG. 2. (Color online) The density of states in the continuum region for N-atom carbon chains sandwiched between two metal electrodes at $V_B = 0.01$ V. Zero energy corresponds to the left Fermi level.

Fano factor [defined as $F_2 = S_2/(2eI)$] is given by

$$F_2 = \frac{\int_{E_{FL}}^{E_{FR}} dE \int d\mathbf{K} |T_L^*(\mathbf{K}) R_R(\mathbf{K})|^2}{\int_{E_{FL}}^{E_{FR}} dE \int d\mathbf{K} |T_R(\mathbf{K})|^2}, \tag{21}$$

where the transmission (reflection) probability (denoted as $T_\mathbf{K}$ and $R_\mathbf{K}$) is related to the transmission (reflection) coefficient [denoted as $T_{L(R)}(\mathbf{K})$ and $R_{L(R)}(\mathbf{K})$] by $T_\mathbf{K} = |T_L(\mathbf{K})|^2$, $R_\mathbf{K} = |R_R(\mathbf{K})|^2 = 1 - T_\mathbf{K}$. Consequently, the shot noise essentially restores the Büttiker-type formula,

$$F_2 = \sum_\mathbf{K} T_\mathbf{K}(1 - T_\mathbf{K}) \Big/ \sum_\mathbf{K} T_\mathbf{K}. \tag{22}$$

In a single-channel tunnel junction with transmission probability T (where the transverse momentum $\mathbf{K}$ is vanishing), moments of the current can be computed by plugging Eqs. (1) and (2) into Eqs. (10), (14), and (18), respectively. It follows that the first, second, and third moment of current are given by $I \propto T$, $S_2 \propto T(1 - T)$, and $S_3 \propto -2T^2(1 - T)$, respectively. The result of the time-unordered third moment is consistent with the results of time-unordered three-current correlations derived by other groups.[29,30] We further define the second- and third-order Fano factors (which are dimensionless) in the small bias regime for steady-state currents as $F_2 = S_2/(2eI)$ and $F_3 = S_3/[(2e)^2 I]$, respectively. For the single-channel junction, $G \propto T$, $F_2 \propto (1 - T)$, and $F_3 \propto -2T(1 - T)$, respectively.

These discussions assume that wave functions are variables separable into the product of components with longitudinal and transverse degrees of freedom. However, the validity of this assumption may be questioned in atomic- or molecular-scale junctions where an abrupt constriction is formed in a nanostructure immediately adjacent to two semi-infinite electrodes with a planar surface. Due to the lack of proper waveguides, the quantization of transverse channels may not be restored in the lead. Consequently, decomposition of the wave function into the product of components with longitudinal and transverse degrees of freedom may not be possible. Moreover, moments of the current are sensitive to the detailed electronic structures in atomic or molecular junctions, making it important to develop formalisms for moments of the current based on the current operator in terms of wave functions. First-principles calculations are therefore performed in the framework of DFT to calculate the current, shot noise, and third moment of the current using Eqs. (10), (14), and (18), respectively. This allows us to investigate the correlation of moments of the current up to the third order at the atomic level using first-principles approaches.

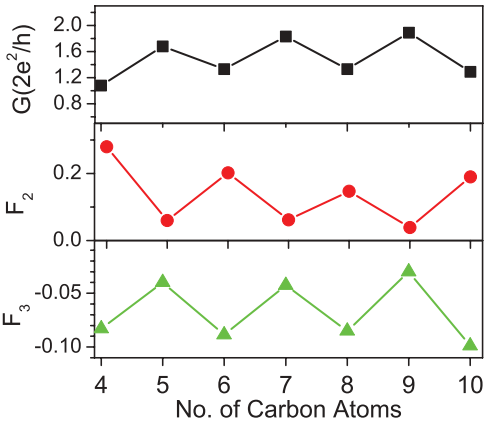

FIG. 3. (Color online) Conductance [(black) square, top panel], the second-order Fano factor [(red) circle, middle panel], and the third-order Fano factor [(green) triangle, bottom panel] of the atomic wires as functions of the number of carbon atoms in the wire at $V_B = 0.01$ V.

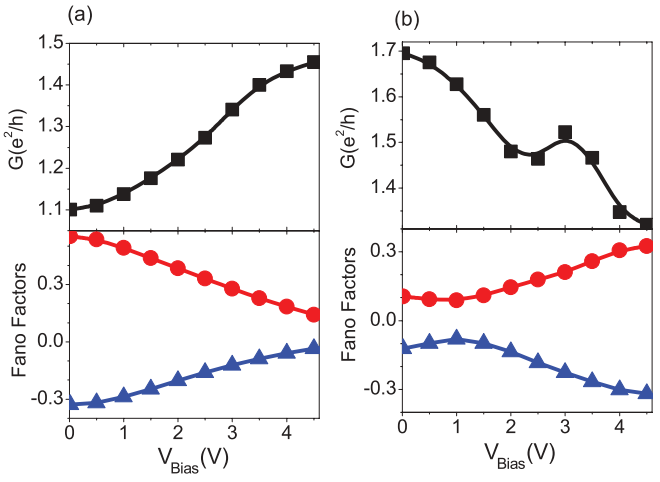

FIG. 4. (Color online) (a) For four-carbon atom wire and (b) for five-carbon atom wire: the differential conductance [(black) square, top panel], the second-order differential Fano factor [(red) circle, bottom panel], and the three-order differential Fano factor [(blue) triangle, bottom panel] vs bias.

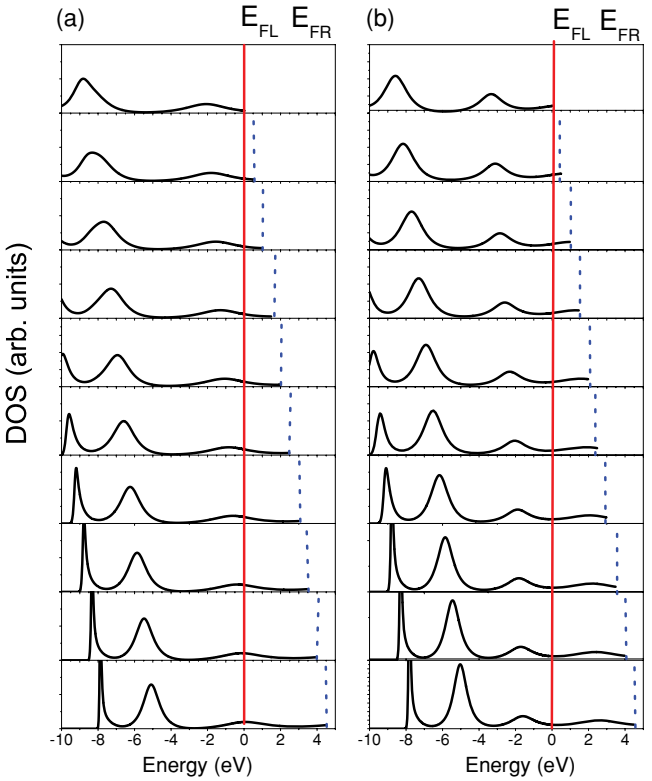

FIG. 5. (Color online) The density of states for various source-drain biases for the (a) C4 atom chain and (b) C5 atom chain for $V_B = 0.1, 0.5, 1.0, 1.5, 2.0, 2.5, 3.0, 3.5, 4.0, 4.5$ V. The left Fermi level E_{FL} (red-dashed lines) is set to be the zero of energy. The right Fermi level E_{FR} (blue-dotted line) defines $V_B = (E_{FR} - E_{FL})/e$.

As an example, the counting statistics is investigated in linear atomic chains formed by four to ten carbon atoms (denoted as C4 to C10) bridging two metal electrodes modeled as electron jellium ($r_s = 2$). The distance between two neighboring carbon atoms is 2.5 a.u., and the end atoms of the chain are fixed at 1.4 a.u. inside the positive background edge of the electron jellium, as shown in Fig. 1(a). The continuum states near the chemical potential show π^*-orbital characters that are twofold degenerate such that each can hold four electrons, as shown in Fig. 1(b). As found in Ref. 20, when the number of carbon atoms is increased by one, the additional carbon atom provides two valence electrons in the continuum states and two valence electrons localized at the atom, as shown in Fig. 2. Consequently, the odd-numbered chains have higher conductance due to the half filled π^* orbital while even-numbered chains have lower conductance due to a full π^* orbital at the Fermi levels, as shown in the upper panel of Fig. 3. The middle and lower panels of Fig. 3 show the influence of the number of carbon atoms on the second-order F_2 and the third-order Fano factor F_3, respectively, in the linear-response regime ($V_B = 0.01$ V). Both F_2 and $|F_3|$ have smaller values for odd-numbered carbon atom chains and larger values for even-numbered atom chains. The π^* orbital causes the oscillation of moments of the current as a function of the number of carbon atoms.

To better understand the relationship among moments of counting statistics in the carbon atom chains, we investigated the differential conductance (defined as $G = \partial I/\partial V$), the differential second-order Fano factor [defined as $F_2 = (1/2e)\partial S_2/\partial I$], and the differential third-order Fano factor [defined as $F_3 = (1/2e)^2\partial S_3/\partial I$] for the C4 and C5 wires (the representative even- and odd-numbered chains) in the nonlinear-response regime. The differential conductance of the C4 chain increases as the applied bias increases, while the differential conductance of the C5 chain decreases as the applied bias increases, as shown in the top panels of Figs. 4(a) and 4(b), respectively. The increase (decrease) of differential conductance with the biases for the C4 (C5) chain is due to the half filled (full) π^* orbital at the Fermi level, where more (less) states are included in the current-carrying energy window created by increasing biases, as shown in Figs. 5(a) and 5(b). The bottom panels of Figs. 4(a) and 4(b) show that conductance and F_3 are strongly positively correlated, inferring that the dominant eigenchannels for counting statistics have transmission probabilities $T > 0.5$.

IV. CONCLUSIONS

Higher moments of the current provide deeper insight into the quantum statistics of charge dynamics, making them more refined tools to characterize the signature of molecules in junctions. Moments of the current in the atomic system are characterized by the wave nature of the current operator in terms of wave functions. The size of nanojunctions are typically smaller than the dephasing length, thus the current operator in this study is expressed in terms of the wave functions. This could lead to interference due to the wave nature of the current operator, which is different from mesoscopic junctions, in which the scattering electrons are incoherent and where the current operator is typically expressed in terms of the scattering matrix.

To illustrate the role of interference effect among wave functions labeled with different transverse momenta $\mathbf{K}$, a theory is developed to calculate the moments of the current until the third order, based on the current operator in terms of wave functions, which are calculated self-consistently in the framework of DFT. We observe that the first moment (current) does not involve the spatial integral of the product of wave functions labeled with different transverse momenta $\mathbf{K}$. This is in sharp contrast to the second and third moments of the current, where the integrals over space mix up the product of wave functions labeled with different transverse momenta $\mathbf{K}$.

The relationships of the conductance, the second, and the third moment of the current are investigated for carbon atom chains of various lengths bridging two metal electrodes in the linear and nonlinear regimes. Moments of the current are shown to be sensitively related to the detailed electronic structures in the atomic and molecular junctions. The carbon atom chains have regularly patterned electronic structures as a function of the number of carbon atoms. Patterned electronic structures serve as ideal test beds in studying the relationship among moments of the current. The carbon monatomic junctions serve as well-defined systems suitable for studying how moments of the current are related to the detailed electronic

structures of nanojunctions. In the linear-response regime, conductance, second, and third moments show odd-even oscillations with the number of carbon atoms, mainly due to the orderly patterned electronic structures of carbon atom chains. In the nonlinear regime, conductance increases (decreases) as bias increases in even- (odd-) numbered carbon atom chains. The F_3 and differential conductances are significantly positively correlated.

Electron-vibration interactions are known to create small structures on the shot-noise profile when the bias is large, giving rise to electrons that have sufficient energy to excite molecular vibration. Similar effects on the third moment of the current are to be investigated in the future.

ACKNOWLEDGMENTS

The authors thank Ministry of Education, Aiming for Top University Plan (MOE ATU), National Center for High-Performance Computing, National Center for Theoretical Sciences (South), and National Science Council (Taiwan) for support under Grants No. NSC 97-2112-M-009-011-MY3, No. 098-2811-M-009-021, and No. 97-2120-M-009-005, and M. Di Ventra and G. B. Lesovik for useful discussions.

*yuchangchen@mail.nctu.edu.tw

[1] A. Aviram and M. A. Ratner, Chem. Phys. Lett. **29**, 277 (1974).
[2] M. Di Ventra, *Electrical Transport in Nanoscale Systems* (Cambridge University Press, Cambridge, England, 2008).
[3] For a review, see Y. M. Blanter and M. Büttiker, Phys. Rep. **336**, 1 (1998).
[4] W. Schottky, Ann. Phys. (Leipzig) **57**, 541 (1918).
[5] M. Büttiker, Y. Imry, R. Landauer, and S. Pinhas, Phys. Rev. B **31**, 6207 (1985).
[6] D. Djukic and J. M. van Ruitenbeek, Nano Lett. **6**, 789 (2006).
[7] P. J. Wheeler, J. N. Russom, K. Evans, N. S. King, and D. Natelson, Nano Lett. **10**, 1287 (2010).
[8] M. Reznikov, M. Heiblum, H. Shtrikman, and D. Mahalu, Phys. Rev. Lett. **75**, 3340 (1995).
[9] N. Agraït, A. L. Yeyati, and J. M. van Ruitenbeek, Phys. Rep. **377**, 81 (2003).
[10] J. Koch and F. von Oppen, Phys. Rev. Lett. **94**, 206804 (2005).
[11] F. Haupt, T. Novotný, and W. Belzig, Phys. Rev. Lett. **103**, 136601 (2009).
[12] T. L. Schmidt and A. Komnik, Phys. Rev. B **80**, 041307(R) (2009).
[13] Y. C. Chen and M. Di Ventra, Phys. Rev. B **67**, 153304 (2003).
[14] J. Lagerqvist, Y. C. Chen, and M. Di Ventra, Nanotech. **15**, S459 (2004).
[15] Y. C. Chen and M. Di Ventra, Phys. Rev. Lett. **95**, 166802 (2005).
[16] J. Yao, Y. C. Chen, M. Di Ventra, and Z. Q. Yang, Phys. Rev. B **73**, 233407 (2006).
[17] M. Kiguchi, O. Tal, S. Wohlthat, F. Pauly, M. Krieger, D. Djukic, J. C. Cuevas, and J. M. van Ruitenbeek, Phys. Rev. Lett. **101**, 046801 (2008).
[18] Y. Kim, H. Song, D. Kim, T. Lee, and H. Jeong, ACS Nano **4**, 4426 (2010).
[19] C. Jin, H. Lan, L. Peng, K. Suenaga, and S. Iijima, Phys. Rev. Lett. **102**, 205501 (2009).
[20] N. D. Lang and Ph. Avouris, Phys. Rev. Lett. **81**, 3515 (1998).
[21] G. B. Bachelet, D. R. Hamann, and M. Schlüter, Phys. Rev. B **26**, 4199 (1982).
[22] M. Di Ventra and N. D. Lang, Phys. Rev. B **65**, 045402 (2001).
[23] N. D. Lang, Phys. Rev. B **52**, 5335 (1995).
[24] J. Taylor, H. Guo, and J. Wang, Phys. Rev. B **63**, 245407 (2001).
[25] K. S. Thygesen and A. Rubio, Phys. Rev. B **77**, 115333 (2008).
[26] G. Vignale and M. Di Ventra, Phys. Rev. B **79**, 014201 (2009).
[27] N. Sai, M. Zwolak, G. Vignale, and M. Di Ventra, Phys. Rev. Lett. **94**, 186810 (2005).
[28] R. Kubo, M. Toda, and N. Hashitsume, *Statistical Physics II: Nonequilibrium Statistical Mechanics* (Springer-Verlag, New York, 1992).
[29] J. Salo, F. W. J. Hekking, and J. P. Pekola, Phys. Rev. B **74**, 125427 (2006).
[30] S. Bachmann, G. M. Graf, and G. B. Lesovik, J. Stat. Phys. **138**, 333 (2010).